

# A Rapid and Facile Synthesis Method for Nanosize Rutile Phase TiO<sub>2</sub> with High Photocatalytic Activity

Priyanka P. Bidaye\*, Julio B. Fernandes

Department of Chemistry, Goa University, Taleigao Plateau, Goa, India

Email: \*bidayepriyanka@gmail.com

**How to cite this paper:** Bidaye, P.P. and Fernandes, J.B. (2019) A Rapid and Facile Synthesis Method for Nanosize Rutile Phase TiO<sub>2</sub> with High Photocatalytic Activity. *Green and Sustainable Chemistry*, 9, 27-37.

<https://doi.org/10.4236/gsc.2019.92003>

**Received:** April 5, 2019

**Accepted:** May 13, 2019

**Published:** May 16, 2019

Copyright © 2019 by author(s) and Scientific Research Publishing Inc.

This work is licensed under the Creative Commons Attribution International License (CC BY 4.0).

<http://creativecommons.org/licenses/by/4.0/>



Open Access

## Abstract

A green, rapid and facile method for synthesis of pure rutile TiO<sub>2</sub> has been developed. Rutile TiO<sub>2</sub> of high purity was synthesized by controlled hydrolysis of TiCl<sub>3</sub> in aqueous medium at room temperature. Addition of nitric acid to TiCl<sub>3</sub> greatly increased the rate of TiCl<sub>3</sub> hydrolysis, crystallization and surface area of the prepared TiO<sub>2</sub> powder. The phase obtained in this way was identified by X-ray diffraction. TiO<sub>2</sub> synthesized by this method showed a unique flower-like assembly of nanotubes, very high surface area and high photocatalytic activity under visible light irradiation.

## Keywords

TiCl<sub>3</sub>, Hydrolysis, Rutile, Nitric Acid, Photocatalytic Activity

## 1. Introduction

Titanium dioxide is a versatile material with a range of applications associated with its unique optoelectronic and photochemical properties such as high refractive index, high dielectric constant, and excellent optical transmittance in the visible and near IR regions as well as its high performance as a photocatalyst [1]. Since TiO<sub>2</sub> is chemically and biologically inert, photocatalytically stable, easy to produce and use without risks to environment and human, it is the well-researched material for wastewater treatment from industries, factories, laboratories, degradation of textile dyes, pesticides and antimicrobial studies [2] [3] [4].

It exists in three crystalline modifications anatase, rutile and brookite. Anatase and rutile are well-known photocatalysts with anatase generally showing higher photocatalytic activity [5]. Rutile form of TiO<sub>2</sub> has some advantages over the

anatase form in terms of higher chemical stability, higher refractive index and is also comparable to anatase in application to dye-sensitized solar cells [6]. Applications of brookite are not much investigated probably because it is rarely obtained in a pure form.

Anatase  $\text{TiO}_2$  has been synthesized by different precursors ( $\text{Ti}(\text{O}^n\text{Bu})_4$ ,  $\text{Ti}(\text{O}^i\text{Pr})_4$ ,  $\text{TiCl}_4$ ,  $\text{TiCl}_3$ ,  $\text{Ti}(\text{SO}_4)_2$  and by different synthesis routes such as hydrothermal, thermohydrolysis and sol-gel process. Among the different methods of synthesis, the sol-gel method is considered advantageous and reproducible one as it leads to nanoparticles of high surface area [7].

Rutile is generally obtained by calcination of the first crystallized anatase at temperatures higher than  $500^\circ\text{C}$ . Direct formation of rutile is possible through long term aging of sols or exposure to high relative humidity or by direct hydrolysis of inorganic salts such as titanium tetrachloride ( $\text{TiCl}_4$ ) in aqueous solutions under hydrothermal or moderate conditions [8].

Anatase  $\text{TiO}_2$  was mostly studied for photocatalytic degradation but lately Rutile  $\text{TiO}_2$  has also shown promising results in photocatalytic studies. The high photocatalytic activity of rutile  $\text{TiO}_2$  for decomposition of rhodamine-B in water is reported under artificial solar light irradiation [9]. Basca and Kiwi found that the presence of rutile  $\text{TiO}_2$  showed enhanced catalytic activity compared to pure anatase  $\text{TiO}_2$  during degradation of p-coumaric acid [10]. Rutile phase has also seen to be more active than anatase in photodecomposition of  $\text{H}_2\text{S}$  and photodecomposition of  $\text{H}_2\text{O}$  [11] [12]. The photovoltaic characteristics of rutile  $\text{TiO}_2$  based DSSCs were found to be comparable to those of anatase  $\text{TiO}_2$ -based solar cells [13] [14].

The present investigation is aimed to synthesize pure rutile phase photoactive Titania by a simplified procedure. Rutile is generally obtained by calcination of the first crystallized anatase at temperatures higher than  $500^\circ\text{C}$  or by doping it with cations such as ( $\text{Li}^+$ ,  $\text{Al}^{3+}$ ,  $\text{Zn}^{2+}$ ,  $\text{K}^+$ ,  $\text{Na}^+$ ) [15] [16]. Direct formation of rutile is possible through long term aging of sols or exposure to high relative humidity or by direct hydrolysis of inorganic salts such as titanium tetrachloride ( $\text{TiCl}_4$ ) in aqueous solutions under hydrothermal or moderate conditions or by using nano rutile as the seed [8] [17]. Photoactive rutile  $\text{TiO}_2$  nanorods have been synthesized using titanium bis (ammonium lactate) dihydroxide as precursor by hydrothermal method and by decorating with anatase nanoparticles [18]. Controlled synthesis of rutile  $\text{TiO}_2$  microspheres, nanoflowers, nanotubes, nanobelts and single crystal rutile  $\text{TiO}_2$  nanotube/nanorod arrays is reported, via acid-hydrothermal synthesis [19].

We have earlier reported that  $\text{TiCl}_3$  is a convenient precursor to obtain  $\text{TiO}_2$  through a solid state decomposition route [20]. Recently  $\text{TiCl}_3$  hydrolysis method has been investigated in detail for the synthesis of  $\text{TiO}_2$  owing to simplicity of  $\text{TiCl}_3$  hydrolysis method.  $\text{TiO}_2$  nanoparticles have been synthesized by hydrolysis and oxidation of  $\text{TiCl}_3$  at  $60^\circ\text{C}$  in aqueous medium through mixed phenomena of precipitation and oxidation by varying the pH of the precursor between 0.5 pH and 6.5 pH [21]. 1d nano rutile  $\text{TiO}_2$  has been synthesized by interfacial

reaction using  $\text{TiCl}_3$  and benzoyl peroxide by hydrothermal treatment at  $80^\circ\text{C}$  for 6 hours [22]. Rutile  $\text{TiO}_2$  was also obtained by direct oxidation of  $\text{TiCl}_3$  [23]. The synthesis of rutile Titania by hydrothermal method using titanium isopropoxide has also been reported [24]. Flower-like rutile Titania nanocrystals were obtained via aqueous phase stirring of  $\text{TiCl}_4$  and  $\text{HCl}$  at low temperature [25]. However,  $\text{TiCl}_4$  is highly hazardous to handle as it fumes easily and hence not considered here.

The research to produce one step synthesis of anatase or rutile nanocrystalline powder at low temperature is of considerable significance. We hereby report for the first time rapid synthesis of photoactive pure rutile phase  $\text{TiO}_2$  by hydrolysis of  $\text{TiCl}_3$  in  $\text{HNO}_3$  medium at  $25^\circ\text{C}$  without using any harsh experimental conditions.

## 2. Experimental

### 2.1. Catalyst Synthesis

A titanium trichloride solution in  $\text{HCl}$  (15%) was taken in a beaker and  $\text{HNO}_3$  was added to it, till the colour of  $\text{TiCl}_3$  changed from violet to colourless. To this distilled water was added such that the ratio of  $\text{TiCl}_3$  and water was 1:9 (V/V). The resulting mixture was then kept on a magnetic stirrer for hydrolysis at room temperature. Hydrolysis of  $\text{TiCl}_3$  in presence of nitric acid was complete in 10 hours. The obtained precipitate was washed free of chloride ions and calcined at  $400^\circ\text{C}$  for 3 h. This sample was named as A1. A blank was kept with the same ratio as  $\text{TiCl}_3$  and water (1:9) but without the addition of  $\text{HNO}_3$ . It took 48 hours for  $\text{TiCl}_3$  hydrolysis in the absence of nitric acid medium.

### 2.2. Catalytic Activity Test

The photocatalytic activity of synthesized sample was investigated for the degradation of methylene blue dye ( $10^{-4}\text{ M}$ ) and congo red dye ( $3.5 \times 10^{-6}\text{ M}$ ) using synthesized catalyst A1 and Degussa (Evonik) P-25 as a standard reference catalyst as per the procedure reported earlier [20]. The experiments were carried out simultaneously for both the catalysts in bright sunlight between 10.00 a.m. to 12.00 noon. Experiments were repeated simultaneously on three different days in order to confirm the consistency of results. In a typical run 50 mL of aqueous dye solution and 0.1 g of the activated catalyst was exposed to sunlight for the duration of the experiment. The solutions thus exposed to sunlight were stirred intermittently. After every 30 minutes, 2 mL aliquots were pipetted out, centrifuged and the absorbance of the clear supernatants was determined at 660 nm and 400 nm wavelength for methylene blue and congo red respectively against appropriate blanks using spectrophotometer.

### 2.3. Characterization

Thermogravimetric analysis (TGA) and differential thermal analysis (DTA) of precursors were carried out on Shimadzu DTG-60 thermal analyzer. The X-ray powder diffraction patterns (XRD) have been recorded on a Rigaku powder

X-Ray diffractometer (Mini Flex II) with Cu K $\alpha$  radiation at a scanning speed of 2°/min. The crystallite size was determined by Scherrer's formula,  $t = (0.9 \lambda / \beta \cos \theta)$  where  $\lambda$  is the wavelength characteristic of the Cu K $\alpha$  radiation,  $\beta$  is the full width at half maximum (in radians) and  $\theta$  is the angle at which 100 intensity peak appears. The BET surface area was measured by N<sub>2</sub> adsorption-desorption method on a Micromeritics Tristar 3000. FEI (model Tecnai F30) high resolution transmission electron microscope (HRTEM) operating at 300 kV was used for TEM measurements. The absorption edges and band gaps were determined from the onset of diffuse reflectance spectra of the samples measured using UV-VIS spectrophotometer (Shimadzu UV-2450).

### 3. Results and Discussions

#### 3.1. Characterization of Materials

##### 3.1.1. Thermogravimetric Analysis

TG-DTA thermogram of the white precursor obtained by hydrolysis reaction of TiCl<sub>3</sub> with nitric acid is given in **Figure 1**. It is clear from the TG profile that the decomposition of the precursor is completed between 300°C - 400°C. The weight loss at 120°C is indicative of loss of water owing to partial dehydroxylation of the OH groups.

##### 3.1.2. X-Ray Analysis

The XRD pattern of the synthesized sample is shown in **Figure 2**. The diffraction

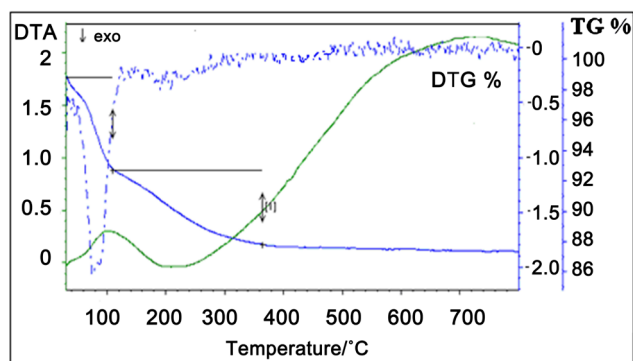


**Figure 1.** Thermogravimetric and differential thermal analysis curves of the precursor for A1.

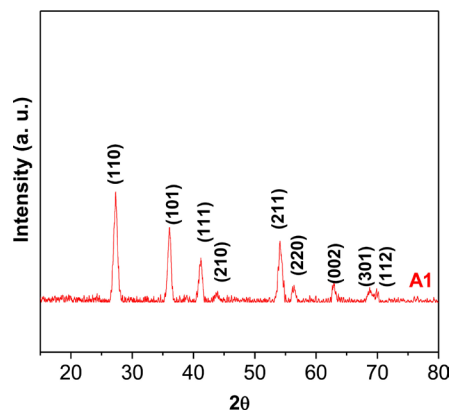


**Figure 2.** XRD pattern of the synthesized catalyst A1.

peaks in this pattern can be indexed to rutile phase [JCPDS No. 76-1940]. Thus, sample A1 obtained by precipitation of  $\text{TiCl}_3$  in presence of nitric acid respectively, showed pure rutile phase.

**Table 1** describes the synthesis of rutile phase Titania and its structural features. As evident from **Table 1**, hydrolysis of  $\text{TiCl}_3$  in presence of nitric acid was complete in 10 hours (A1) as compared to the blank that took 48 hours. It is noted from literature [26] that relatively fast hydrolysis of  $\text{TiCl}_3$  in presence of  $\text{H}_2\text{O}$  is possible only at elevated temperatures. It has been observed that the ratio inorganic precursor: Water: $\text{HNO}_3$  is an important factor for controlling the rate of hydrolysis and phase formation. In  $\text{TiO}_2$  rutile structure, (110) plane is the most thermodynamically stable and the growth rate of the plane (110) occurs faster compared to other planes [19]. Thus rutile  $\text{TiO}_2$  is formed in the stable  $\text{Ti}^{4+}$  acidic solution. In the present investigation a simple and rapid method is reported, to obtain  $\text{TiO}_2$  from aqueous solutions of  $\text{TiCl}_3$  at room temperature. The surface area of A1 is also significantly higher than Degussa (Evonik) P-25 (**Table 1**).

### 3.1.3. HRTEM Analysis

HRTEM micrographs of the synthesized sample are shown in **Figure 3**. HRTEM images of A1 (synthesized in presence of  $\text{HNO}_3$ ) show the formation of flower-like structures. It reveals that these structures are a unique assembly of nanoflowers like structures with  $\sim 40$  nm length and 10 - 15 nm diameter. It is observed that the reported synthesis process has a capability to produce self organized nanostructures with flower-like morphology without use of any templating agent.

**Table 1.** Synthesis and structural features of titania samples.

| Sr. No. | Code                  | Method  | Hydrolysis time | %yield | % Rutile | Scherrer's crystallite sizes (nm) | BET surface area ( $\text{m}^2/\text{g}$ ) |
|---------|-----------------------|---|-----------------|--------|----------|-----------------------------------|--|
| 1       | A1                    | $\text{TiCl}_3:\text{H}_2\text{O}:\text{HNO}_3$ | 10 hrs          | 100    | 100      | 16                                | 103  |
| 2       | Degussa (Evonik) P-25 |   |                 |        | 16       | 20.59                             | 50   |

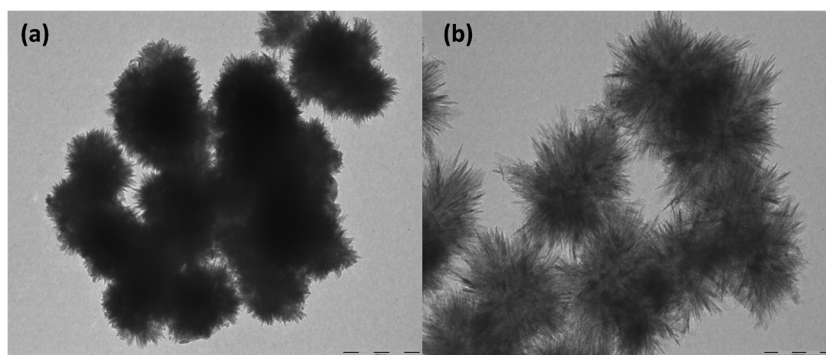


**Figure 3.** TEM image of A1 synthesized by hydrolysis of  $\text{TiCl}_3$  in presence of  $\text{HNO}_3$  (Scale represents (a) 500 nm, (b) 200 nm).

The formation of nanoflower structured rutile  $\text{TiO}_2$  may be related to the synthesis method applied in the procedure. The oxidation of the  $\text{TiCl}_3$  (in 15% HCl solution) with  $\text{HNO}_3$  produces  $\text{Ti}^{4+}$  ions in the aqueous acidic solution. The hydrolysis of  $\text{Ti}^{4+}$  ions in the acidic solutions results in the production of fewer  $\text{TiO}_2$  polycrystalline seeds. Thus the solution consists of supersaturated solution of  $\text{Ti}^{4+}$  ions and fewer polycrystalline  $\text{TiO}_2$  seeds. The crystal growth of seeds into nanorods occurs by the deposition of  $\text{Ti}^{4+}$  ions from the solution on the surface of this polycrystalline seeds. Subsequent crystal growth proceeds to form nanorods along specific directions and then self-assemble into nanoflowers through Ostwald ripening process [19].

### 3.1.4. $\text{N}_2$ Adsorption-Desorption Isotherm

The  $\text{N}_2$  adsorption-desorption isotherms and pore distribution analysis for sample A1 (inset) is given in **Figure 4**. The adsorption-desorption isotherm of the synthesized materials shows Type IV physisorption isotherm with H2 hysteresis loop, which is the characteristic of mesoporous materials [27]. In the isotherm the pore filling step occurs at low relative pressure ( $P/P_0 = 0.44$ ) and also the upper closure point of the hysteresis loop appeared at a relatively lower value of ( $P/P_0 = 0.72$ ) which indicates that the sample contains smaller pores [28]. From pore size distribution it is observed that the pores are small and narrow with uniform pore size of 3.6 nm diameter. Sharp hysteresis loop and narrow pore size distribution in the porosity analysis confirmed the presence of smaller pores which may have formed by the ordered arrangement of nanosize rods of individual nanoflowers.

### 3.1.5. UV-Vis Absorption Study

**Figure 5** shows the UV-Vis absorbance spectra of the synthesized Titania sample. It is clear that the samples showed absorption edge in the visible region (**Table 2**). The band gap of the samples was determined by the equation  $E_g = 1239.8/\lambda$ , where  $E_g$  is the band gap energy (eV) and  $\lambda$  (nm) is the wavelength of the absorption edges in the spectra [29].

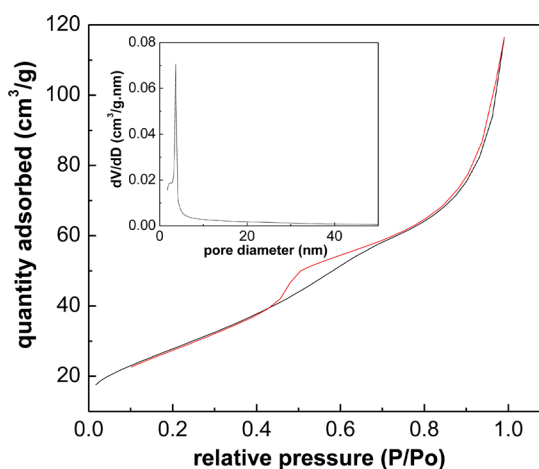


**Figure 4.**  $\text{N}_2$  adsorption-desorption isotherm and BJH pore analysis of A1.

### 3.2. Photocatalysis Study

The percentage degradation profiles of methylene blue and congo red with time are shown in **Figure 6(a)** and **Figure 7(a)** respectively. A1 catalyst showed high photocatalytic activity almost equal as TiO<sub>2</sub> Degussa (Evonik) P-25 catalyst.

The time dependant UV-Vis spectra of methylene blue and congo red dye in presence of catalyst A1 is given in **Figure 6(b)** and **Figure 7(b)** respectively. It is clear from both the figures that the decolourisation of dye precedes with increase in time. A1 obtained by room temperature hydrolysis of TiCl<sub>3</sub> in presence of nitric acid medium showed a 100% rutile phase, yet it showed photocatalytic activity comparable to Degussa (Evonik) P-25 for photodegradation of methylene blue as well as congo red. This is probably the first report of a rutile phase showing such high photocatalytic activity for both cationic dye methylene blue and anionic dye congo red. This excellent photodegradation using A1 can be due to the presence of favorable parameters such as particle size, nanorod shape of the particles, crystalline phase and very high surface area. It also possesses small

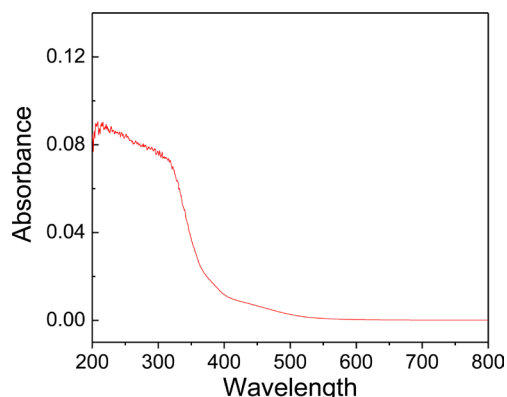


**Figure 5.** UV-Vis absorbance spectra of the catalyst A1.

**Table 2.** The calculated band gaps of the Titania samples.

| Catalyst      | A1   | Degussa (Evonik) P-25 |
|---------------|------|-----------------------|
| Band gap (eV) | 2.88 | 2.97                  |

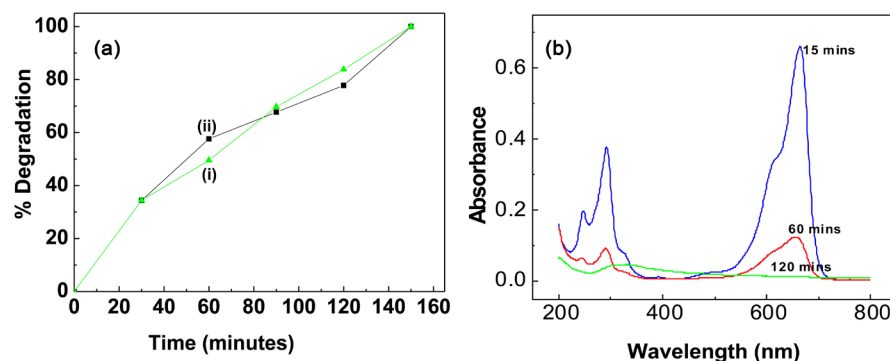


**Figure 6.** (a) Percentage degradation of methylene blue with time during photocatalysis using (i) A1, (ii) Degussa (Evonik) P-25; (b) Time dependent UV-Vis spectra of methylene blue in presence of catalyst A1.

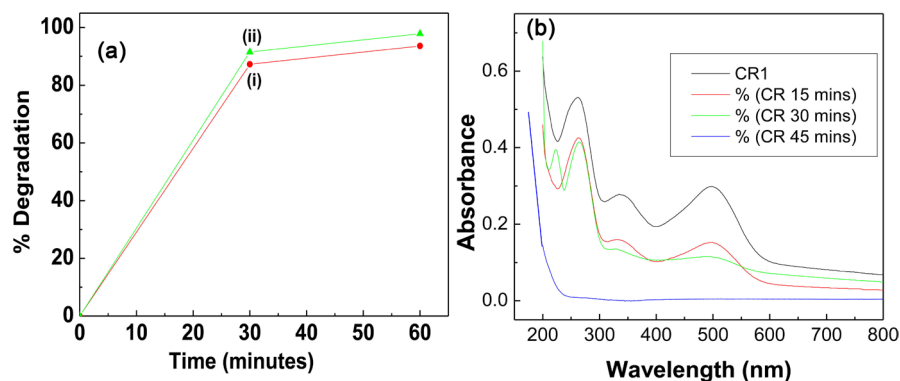


**Figure 7.** (a) Percentage degradation of congo red with time during photocatalysis using (i) A1, (ii) Degussa (Evonik) P-25; (b) Time-dependent UV-Vis spectra of congo red in presence of catalyst A1.

band gap (2.88) in comparison to the reported band gap of Degussa (Evonik) P-25 (3.14). It is earlier reported that for each titanium dioxide phase, some optimum size and shape exists where each phase presents high photocatalytic activity [30]. Thus, this investigation resulted in rapid synthesis of a nano rutile catalyst having excellent efficiency for degradation of methylene blue as well as congo red. The photocatalytic process mainly occurs on the surface of the photocatalyst and adsorption precedes photodegradation [31]. As seen from **Table 1** catalyst A1 had a high surface area and a smaller crystallite size. Other factors such as narrow pore size distribution and lower band gap could have facilitated the adsorption and degradation of the dye in the visible region with enhanced photocatalytic activity comparable to that of Degussa (Evonik) P-25.

#### 4. Conclusions

- $\text{TiO}_2$  can be rapidly synthesized at room temperature from aqueous solutions of  $\text{TiCl}_3$  in presence of nitric acid;
- Controlled hydrolysis of  $\text{TiCl}_3$  yields pure rutile phase  $\text{TiO}_2$  with high surface area having flower-like assembly of nanosized rods;
- Rutile  $\text{TiO}_2$  synthesized by a simple hydrolysis method showed excellent efficacy for degradation of cationic dye methylene blue as well as anionic dye congo red in the visible light;
- The ease of synthesis makes it an attractive and promising catalyst and its efficiency could further be explored for DSSC's, water splitting, photocatalytic reduction of  $\text{CO}_2$ , etc. in future studies.

#### Acknowledgements

The authors are grateful for the financial support received from DST Nano Mission program, SR/NM/NS-86/2009.

#### Conflicts of Interest

The authors declare no conflicts of interest regarding the publication of this paper.



## References

- [1] Diebold, U. (2003) The Surface Science of Titanium Dioxide. *Surface Science Reports*, **48**, 53-229. [https://doi.org/10.1016/S0167-5729\(02\)00100-0](https://doi.org/10.1016/S0167-5729(02)00100-0)
- [2] Silva, C.G., Wang, W. and Faria, J.L. (2006) Photocatalytic and Photochemical Degradation of Mono-, Di- and Tri-Azo Dyes in Aqueous Solution under UV Irradiation. *Journal of Photochemistry and Photobiology A: Chemistry*, **181**, 314-324. <https://doi.org/10.1016/j.jphotochem.2005.12.013>
- [3] Allen, N.S., Edge, M., Verran, J., Caballero, L., Abrusci, C., Stratton, J., Maltby, J. and Bygott, C. (2009) Photocatalytic Surfaces: Environmental Benefits of Nanotitania. *The Open Materials Science Journal*, **3**, 6-27. <https://doi.org/10.2174/1874088X00903010006>
- [4] Ahmed, O.B. (2018) Evaluation of the Antimicrobial Efficacy of Titanium Dioxide Nanoparticles on the Surfaces of Public Toilets. *Green and Sustainable Chemistry*, **8**, 32-38. <https://doi.org/10.4236/gsc.2018.81003>
- [5] Linsebigler, A.L., Lu, G. and Yates Jr., J.T. (1995) Photocatalysis on TiO<sub>2</sub> Surfaces: Principles, Mechanisms and Selected Results. *Chemical Reviews*, **95**, 735-758. <https://doi.org/10.1021/cr00035a013>
- [6] Chen, X. and Mao, S.S. (2007) Titanium Dioxide Nanomaterials: Synthesis, Properties, Modifications, and Applications. *Chemical Reviews*, **107**, 2891-2959. <https://doi.org/10.1021/cr0500535>
- [7] Parra, R., Goes, M.S., Castro, M.S., Longo, E., Bueno, P.R. and Varela, J.A. (2008) Reaction Pathway to the Synthesis of Anatase via the Chemical Modification of Titanium Isopropoxide with Acetic Acid. *Chemistry of Materials*, **20**, 143-150. <https://doi.org/10.1021/cm702286e>
- [8] Hosono, E., Fujihira, S., Kakiuchi, K. and Imai, H. (2004) Growth of Submicrometer-Scale Rectangular Parallelepiped Rutile TiO<sub>2</sub> Films in Aqueous TiCl<sub>3</sub> Solutions under Hydrothermal Conditions. *Journal of the American Chemical Society*, **126**, 7790-7791. <https://doi.org/10.1021/ja048820p>
- [9] Wang, Y., Zhang, L., Deng, K. and Zhou, Z. (2007) Low Temperature Synthesis and Photocatalytic Activity of Rutile TiO<sub>2</sub> Nanorod Superstructures. *Journal of Physical Chemistry C*, **111**, 2709-2714. <https://doi.org/10.1021/jp066519k>
- [10] Baca, R.R. and Kiwi, J. (1998) Effect of Rutile Phase on the Photocatalytic Properties of Nanocrystalline Titania during the Degradation of p-Coumaric Acid. *Applied Catalysis B: Environmental*, **16**, 19-29. [https://doi.org/10.1016/S0926-3373\(97\)00058-1](https://doi.org/10.1016/S0926-3373(97)00058-1)
- [11] Beck, D.D. and Siegel, R.W. (1992) The Dissociative Adsorption of Hydrogen Sulfide over Nanophase Titanium Dioxide. *Journal of Materials Research*, **7**, 2840-2845. <https://doi.org/10.1557/JMR.1992.2840>
- [12] Ohno, T., Haga, D., Fujihara, K., Kaizaki, K. and Matsumura, M. (1997) Unique Effects of Iron(III) Ions on Photocatalytic and Photoelectrochemical Properties of Titanium Dioxide. *The Journal of Physical Chemistry B*, **101**, 6415-6419. <https://doi.org/10.1021/jp971093i>
- [13] Park, N.G., Schlichthorl, G., Lagemaat, J., Cheong, H.M., Mascarenhas, A. and Frank, A.J. (1999) Dye-Sensitized TiO<sub>2</sub> Solar Cells: Structural and Photoelectrochemical Characterization of Nanocrystalline Electrodes Formed from the Hydrolysis of TiCl<sub>4</sub>. *The Journal of Physical Chemistry B*, **103**, 3308-3314. <https://doi.org/10.1021/jp984529i>
- [14] Park, N.G., Lagemaat and Frank, A.J. (2000) Comparison of Dye-Sensitized Rutile-

- and Anatase-Based TiO<sub>2</sub> Solar Cells. *The Journal of Physical Chemistry B*, **104**, 8989-8994. <https://doi.org/10.1021/jp994365l>
- [15] Heald, E.F. and Weiss, C.W. (1972) Kinetics and the Mechanism of the Anatase/Rutile Transformation, as Catalyzed by Ferric Oxide and Reducing Conditions. *American Mineralogist*, **57**, 10-23.
- [16] Talavera, R.R., Vargas, S., Murillo, R.A., Campos, R.M. and Poniatowski, E.H. (1997) Modification of the Phase Transition Temperatures in Titania Doped with Various Cations. *Journal of Materials Research*, **12**, 439-443. <https://doi.org/10.1557/JMR.1997.0065>
- [17] Li, Y., Fan, Y. and Chen, Y. (2002) A Novel Method for Preparation of Nanocrystalline Rutile TiO<sub>2</sub> Powders by Liquid Hydrolysis of TiCl<sub>4</sub>. *Journal of Materials Chemistry*, **12**, 1387-1390. <https://doi.org/10.1039/b200018k>
- [18] Kandiel, T.A., Dillert, R., Feldhoff, A. and Bahneman, D.W. (2010) Direct Synthesis of Photocatalytically Active Rutile TiO<sub>2</sub> Nanorods Partly Decorated with Anatase Nanoparticles. *The Journal of Physical Chemistry C*, **114**, 4909-4915. <https://doi.org/10.1021/jp912008k>
- [19] Zhou, W., Liu, X., Cui, J., Liu, D., Li, J., Jiang, H., Wang, J. and Liu, H. (2011) Control Synthesis of Rutile TiO<sub>2</sub> Microspheres, Nanoflowers, Nanotrees and Nanobelts via Acid Hydrothermal Method and Their Optical Properties. *Crystal Engineering Communication*, **13**, 4557-4563. <https://doi.org/10.1039/c1ce05186e>
- [20] Bidaye, P.P., Khushalani, D. and Fernandes, J.B. (2010) A Simple Method for Synthesis of S-Doped TiO<sub>2</sub> of High Photocatalytic Activity. *Catalysis Letters*, **134**, 169-174. <https://doi.org/10.1007/s10562-009-0217-3>
- [21] Cassaignon, S., Koelsch, M. and Joliver, J.P. (2007) From TiCl<sub>3</sub> to TiO<sub>2</sub> Nanoparticles (Anatase, Brookite and Rutile): Thermohydrolysis and Oxidation in Aqueous Medium. *Journal of Physics and Chemistry of Solids*, **68**, 695-700. <https://doi.org/10.1016/j.jpcs.2007.02.020>
- [22] Li, X., Liu, Y., Li, T. and Zhang, Z. (2006) Synthesis of 1D Nanorutile ( $\alpha$ -TiO<sub>2</sub>) by Interfacially Initiating Redox Reaction at Low Temperature. *Chemistry Letters*, **35**, 898-899. <https://doi.org/10.1246/cl.2006.898>
- [23] Pedraza, F. and Vasquez, A. (1999) Obtention of TiO<sub>2</sub> Rutile at Room Temperature through Direct Oxidation of TiCl<sub>3</sub>. *Journal of Physics and Chemistry of Solids*, **60**, 445-448. [https://doi.org/10.1016/S0022-3697\(98\)00315-1](https://doi.org/10.1016/S0022-3697(98)00315-1)
- [24] Aruna, S.T., Tirosh, S. and Zaban, A. (2000) Nanosize Rutile Titania Particle via a Hydrothermal Method without Mineralizers. *Journal of Materials Chemistry*, **10**, 2388-2391. <https://doi.org/10.1039/b001718n>
- [25] Li, Y., Liu, J. and Jia, Z. (2006) Morphological Control and Photodegradation Behavior of Rutile TiO<sub>2</sub> Prepared by a Low-Temperature Process. *Materials Letters*, **60**, 1753-1757. <https://doi.org/10.1016/j.matlet.2005.12.012>
- [26] Masuda, Y. and Koumoto, K. (2004) Deposition Mechanism of Anatase TiO<sub>2</sub> from an Aqueous Solution and Its Site-Selective Deposition. *Solid State Ionics*, **172**, 283-288. <https://doi.org/10.1016/j.ssi.2004.02.068>
- [27] Sing, K.S.W., Everett, D.H., Haul, R.A.W., Moscou, L., Pierotti, R.A., Rouquerol, J. and Siemieniewska, T. (1985) Reporting Physisorption Data for Gas/Solid Systems with Special Reference to the Determination of Surface Area and Porosity. *Pure and Applied Chemistry*, **57**, 603-619. <https://doi.org/10.1515/iupac.57.0007>
- [28] Cejka, J., Zilkova, N., Rathousky, J. and Zukal, A. (2001) Nitrogen Adsorption Study of Organised Mesoporous Alumina. *Physical Chemistry Chemical Physics*, **3**, 5076-5081. <https://doi.org/10.1039/b105603b>

- [29] Regan, B.O. and Gratzel, M. (1991) A Low-Cost, High-Efficiency Solar Cell Based on Dye-Sensitized Colloidal TiO<sub>2</sub> Films. *Nature*, **353**, 737-740. <https://doi.org/10.1038/353737a0>
- [30] Melghit, K. and Al-Rabaniah, S.S. (2006) Photodegradation of Congo Red under Sunlight Catalysed by Nanorod Rutile TiO<sub>2</sub>. *Journal of Photochemistry and Photobiology A*, **184**, 331-334. <https://doi.org/10.1016/j.jphotochem.2006.05.004>
- [31] Gandhe, A.R. and Fernandes, J.B. (2005) A Simple Method to Synthesize N-Doped Rutile Titania with Enhanced Photocatalytic Activity in Sunlight. *Journal of Solid State Chemistry*, **178**, 2953-2957. <https://doi.org/10.1016/j.jssc.2005.06.034>